IOP Conf. Series: Materials Science and Engineering **449** (2018) 012004 doi:10.1088/1757-899X/449/1/012004

Theoretical Study of A Three-Swing Blades Rotary Engine

H.K. Ma[1*], N.T. Liu[1], M.H. Hsu[2], Y.W. Liu[2] and C.Y. Lin[2]

[1]Research Center of Climate Change & Sustainable Development, National Taiwan University, Taiwan
[2]Mechanical Engineering Dept., National Taiwan University, Taiwan

[*]Email: skma@ntu.edu.tw

Abstract. The innovative eccentric swing blade rotary engine is internally divided into a compression section, a combustion chamber, and a power section. With the three swing blades on each rotor, the swing blade comprises a cylindrical roller mounted to a front end and a curved back, and each of the roller is provided, at an inner side, with a support device that is capable of sustaining a counteracting force applied by a cylinder wall to the roller. After completing the combustion of the mixed gas in the combustion chamber, the generated high-pressure gas is injected into power section and push the swing blades rotation, resulting in power. In this study, the theoretical model has been established to calculate the trajectory/the tip speed of the swing blade, pressure variation, compression torque and to predict the performance of the rotary engine. For a prototype 120 cc rotary engine, it can provide an estimated power output between 6.26 to 50.16-hp at about 1000 to 8000 rpm.

1. Introduction

Invented in 1933 by Felix Wankel, the Wankel rotary engine was used in many famous automotive manufactures like Toyota, Daimler Benz and General Motor etc. Previously, Mazda, former Toyo Kogyo [1], had launched many commercial vehicles form RX-3 to RX-8 which provides up to 247-hp with its RENESIS engine. Although having advantages like lower vibration, smaller engine size and weight, the Wankel engine suffers from higher fuel consumption and maintenance issues. Through the optimization of combustion, the rotary engines are now being used on small UAVs of some countries, providing an estimated power output between 20 and 90-hp [2]. One Research has also proved the viability through real manufacturing, making a 35.6kg Wankel engine prototype providing 55-hp at about 8000 rpm [3]. Recently, a new form of powertrain that is lightweight and small size will have numerous applications in motor cycles, unmanned aerial vehicles and the automotive industry. The Mazda2/3/CX-3, Chevrolet Volt and BMW i3 have announced new range extenders driving an electric generator which charges a battery to supply the vehicle's electric motor with electricity. Due to the compact size and the high power to weight ratio of a Wankel engine, it has been used for electric vehicles as range extenders to provide supplementary power [4]. In this study, an innovative eccentric swing blade rotary engine with three swing blades has been developed and internally divided into a compression section, a combustion chamber, and a power section [5-6]. Also, the theoretical model has been established to calculate the trajectory/the tip speed of the swing blade, pressure variation, compression torque and to predict the performance of the rotary engine.

2. Actuation principle of an eccentric swing blade rotary engine

The eccentric swing blade rotary engine shown in Figure 1 is comprised of a compression section and a power section each provided with a rotor device. Each rotor device is made up of a rotor body and three swing blades. Each swing blade is pivotally connected to the rotor body and may swing about an axis defined by a pivot pin.

Figure 2 shows the actuation of the eccentric swing blade rotary engine. The swing blades continuously moves and propels the compressed air/fuel mixture into the combustion chamber. When the compressed gas is ignited, the high pressure combustion gas will push the blade and generate power.

Figure 1. An eccentric swing blade rotary engine

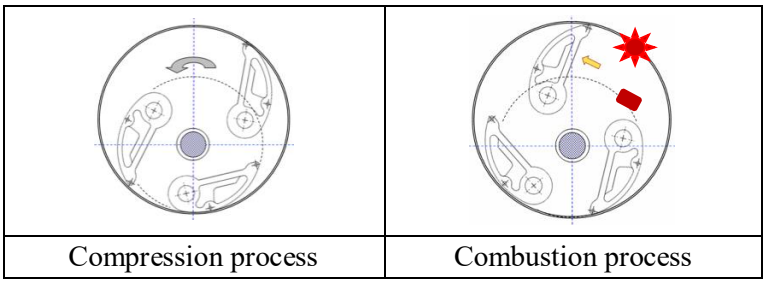

Figure 2. Actuation of the eccentric swing blade rotary engine

3. Analysis of the trajectory of an eccentric swing blade

Table 1. The parameters of 120 cc swing blade rotary engine

Parameter	Definition	Unit (mm)
R	Radius of the cylinder	62.5
r	Radius of the rotor	32
e	Eccentricity of the rotor	12.5
l	Length of the blade	57
H	Height of the cylinder	35

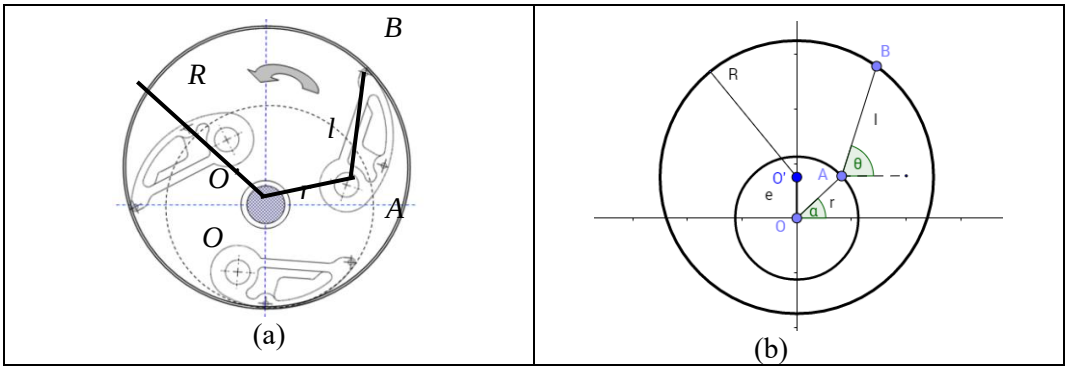

Figure 3. Symbol definition of an eccentric swing blade rotary engine

To establish the theory of eccentric swing blade rotary engine, we construct the model of the engine and make the analysis of the trajectory of the blade. Table 1 shows the parameters of the 120cc swing

blade rotary engine. And, Figure 3 shows the symbol definition of the model. The motion of the swing blade is an "arc" along the cylinder wall.

3.1 The tip trajectory equation and the maximum open of swing blade

The tip of the blade B(x,y) moves along the cylinder, forming an eccentric circle as the trajectory Eqn. (1).

$$-2\mathrm{elsin}(\theta) - 2\mathrm{ersin}(\alpha) + 2\mathrm{lrcos}(\alpha - \theta) = \mathrm{R}^2 - \mathrm{r}^2 - \mathrm{l}^2 - \mathrm{e}^2 \quad (1)$$

The relation of θ and α can be described by Eqn. (1). In the design of 120 cc engine, the modification changes the ratio of the radius of rotor to the radius of cylinder to be 10:8 to adjust the maximum open angle (θ - α). To avoid the stagnation of moving, the open angle (θ - α) ranges from 80° to 130°.

3.2 Pressure variation in the compression section and power section

The estimated maximum volume (TDC) is roughly 120 cc and the minimum volume at BDC is 24 cc by considering the volume of blade (23 cc). The volume of combustion chamber is 10 cc. The designed volume in power section leads the volume in compression section by 30 deg.

The inlet gas pressure is atmospheric pressure $\mathrm{P}_1 = 1.003$ bar and the volume of the working chamber when the compression starts $\mathrm{V}_1 = 120\ \mathrm{C.C.}$ Assuming the process is an isentropic compression process, the pressure variation of the compression section can be obtained from the relation $\mathrm{PV}^{\mathrm{k}} = \mathrm{C}$. Figure 4 shows the pressure variation in both power and compression section, the maximum pressure 4.671 bar is obtained at α = 145° (BDC), which is the pressure in combustion chamber. The pressure at α = 145°~220° is due to the residual gas remained in the compression section. The exhaust and intake begins at α = 220° and ends at α = 300° (TDC) where the compression starts. After heat adding in the combustion chamber, the maximum pressure is 21.68 bar at α = 145°. Isentropic expansion is happened during α = 145°~ 300° . The exhaust port opens at α = 300° (TDC) and closes at next combustion starts.

3.3 The Thermodynamic properties in power cycle

The proportional ratio of CVC and CPC affects the pressure and temperature after combustion. This proportional ratio relates to the open timing of the exhaust port at the outlet of combustion chamber to the power section. Maximum heat can be released shown in Figure 5 during the combustion of octane fuel for the case CVC/CPC=0.6/0.4.

3.4 Torque

$$Torque = \Delta P * h * (\frac{1}{2} l^2 + rl(cos(\theta - \alpha)) \quad (2)$$

ΔP is the pressure difference between two sides of blade and h is the height of compression section. When we only consider the effect of single blade, the variation of torque output is shown in Figure 4. We can notice that the value of torque output is negative in some periods, which means the blade is pushed by the gas and output power. The major reason of this phenomenon is that, in these periods, the compression section ends the connection to the combustion chamber but there is still a small space containing residual high pressure gas between the two adjacent blades. As a result, the high pressure air will push the blade and causes the torque output to have a negative value.

3.5 The influence of combustion chamber on compression section and power section

In this section, Table 2 Summary of power balance with combustion chamber. Also, the influence of combustion chamber and the possible reasons causing the discontinuous points (sudden increase or decrease) are discussed. There are several discontinuous points can be found in Figure 4 (yellow circles). To realize this phenomenon, we compare the pressure variation in front of and behind the blade with the torque output. The red and yellow curves shows the variation of the pressure in front of

and behind the blade respectively. We can realize these are caused by starting and ending the connection between combustion chamber and the compression section. Since the variation of torque output is associated with the variation of pressure, we can confirm that it is the sudden open and closure of combustion chamber make the torque output discontinuous. And then, Figure 5 shows the variation of torque output with respect to (α) for a single blade in power section. Finally, Figure 6 combines the total torque input in compression section and the total torque output in power section. It allows us to derive the total power output by integrating the net torque output with respect to (α), and the effect of a single blade contributing to the total torque output can also be observed in Figure 6.

Table 2. Summary of power balance with combustion chamber

Power	**With combustion chamber**
Power consumption in compression section	9.1887J/round
Power generation in power section	154.6925J/round
Net power output	145.5038J/round

Figure 4. The variation of torque with respect to (α) for a single blade and the variation of the pressure in front of and behind the blade compression section

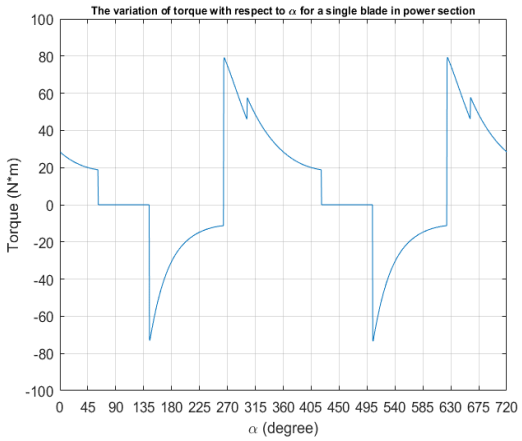

Figure 5. The variation of torque with respect to (α) for a single blade in power section

3.6 Performance of the rotary engine

The performance of swing blade rotary engine can be evaluated by the following formulas in Table 3.

Table 3. The performance of 120 cc swing blade rotary engine

Definition	Formula	Calculated Result	Note
Thermal efficiency	$\eta_{th} = \frac{W_{net}}{Q_{in}}$	63.84%	W_{net} is calculated from PVdiagram
Indicated mean effective Pressure (IMEP)	$P_{imep} = \frac{W_{net}}{V_d}$	2.96~3.75 bar	V_d is the displacement volume (V_{TDC} - V_{BDC})
Indicated horse power	$N_i = \frac{P_{imep} \times V_d \times \omega}{44700}$	6.26~50.16 hp (rpm 1000~8000)	ω : (rpm)
Shaft horse power	$N_s = \frac{W_{torque} \times \omega}{44700}$	2.80~22.38 hp (rpm 1000~8000)	ω : (rpm)
Mechanical efficiency	$\eta_{me} = \frac{N_s}{N_i}$	15.97~44.63%	

Figure 6. The variation of torque with respect to (α) when combining the compression section and the power section, and the area between two curves is the net power output

4. Conclusions

The innovative eccentric swing blade rotary engine with three swing blades has been developed and internally divided into a compression section, a combustion chamber, and a power section. At the same time, the theoretical model has been established to calculate the trajectory/the tip speed of the swing blade, pressure variation, compression torque and to predict the performance of the rotary engine. This study has proved the viability through the cold model test and the predicted results of theoretical model. For a prototype 120 cc rotary engine, it can provide an estimated power output between 6.26 to 50.16-hp at about 1000 to 8000 rpm. The innovative eccentric swing blade rotary engine is only one-fifth of the multi-cylinder piston engine by volume, weighs only one-sixth, which allows the vehicle to operate with higher power intensity, light in weight and low CO_2 emission.

Appendix

A	Axis of the blade
A_{tot}	Area of the working chamber
B	Tip of the blade
D	The distance from the rotor axis to the tip of blade
e	Eccentricity of the rotor
l	Length of the blade
R	Radius of the cylinder
r	Radius of the rotor
α	The angle between the blade axis and horizontal line
θ	The angle between the blade tip and horizontal line ◦
ΔP	The pressure difference between two sides of blade
h	The height of the compression section

Acknowledgments
The study group thanks the Ministry of Science and Technology for funding support (MOST 107-3113-E-002-008-).

References
[1] K. Yamamoto, “Rotary Engine”, Toyo Kegyo Co., Ltd., 1981.
[2] C.B.M. Kweon, “A Review of Heavy-Fueled Rotary Engine Combustion Technologies (OMB No. 0704-0188)”. U.S. Army Research Laboratory, (2011), 15.
[3] K.M. Pillai, A.J.S. Mithran, V.K.W. Grips, K.S. Kumar, U.K. Sinha, M.N. Varadarajan, J.J. Isaac and Y.V.S. Murthy, “Design and development of an indigenous 55 HP Wankel Engine”, *Proceedings of the International Conference on Aerospace Science and Technology,* (2008), 4.
[4] P. Harrop, "Hybrid vehicle range extenders: goodbye pistons". IDTechEx, *Nature America*, 304(1), (2015), 25.
[5] N.T. Liu, US patent no. 6,082,324 , 9,458,719 and Taiwan patent no. I-468581 , I-479075
[6] H.K. Ma, etc, Taiwan patent no.106218131.